Naval Research Laboratory

Washington, DC 20375-5320

Blast Mitigation Using Water Mist: Test Series II

HEATHER D. WILLAUER
RAMAGOPAL ANANTH
JOHN P. FARLEY
FREDERICK W. WILLIAMS

Navy Technology Center for Safety and Survivability
Chemistry Division

GERALD G. BACK

Hughes Associates, Inc.
Baltimore, Maryland

MATTHEW C. KENNEDY
JOHN O'CONNOR

Naval Surface Warfare Center
Indian Head, Maryland

VICTOR M. GAMEIRO

Marioff, Inc.
Linthicum, Maryland

March 12, 2009

REPORT DOCUMENTATION PAGE

1. REPORT DATE (DD-MM-YYYY) 12-03-2009	2. REPORT TYPE Memorandum Report	3. DATES COVERED (From - To)

4. TITLE AND SUBTITLE

Blast Mitigation Using Water Mist: Test Series II

5a. CONTRACT NUMBER

5b. GRANT NUMBER

5c. PROGRAM ELEMENT NUMBER
61-8804

6. AUTHOR(S)

Heather D. Willauer, Ramagopal Ananth, John P. Farley, Frederick W. Williams, Gerald G. Back,* Matthew C. Kennedy,† John O'Connor,† and Victor M. Gameiro‡

5d. PROJECT NUMBER

5e. TASK NUMBER

5f. WORK UNIT NUMBER

7. PERFORMING ORGANIZATION NAME(S) AND ADDRESS(ES)

Naval Research Laboratory, Code 6180
4555 Overlook Avenue, SW
Washington, DC 20375-5320

8. PERFORMING ORGANIZATION REPORT NUMBER

NRL/MR/6180--09-9182

9. SPONSORING / MONITORING AGENCY NAME(S) AND ADDRESS(ES)

Office of Naval Research
One Liberty Center
875 North Randolph Street
Arlington, VA 22203-1995

10. SPONSOR / MONITOR'S ACRONYM(S)

11. SPONSOR / MONITOR'S REPORT NUMBER(S)

12. DISTRIBUTION / AVAILABILITY STATEMENT

Approved for public release; distribution is unlimited.

13. SUPPLEMENTARY NOTES

*Hughes Associates, Inc., Baltimore, MD
†Naval Surface Warfare Center, Indian Head, MD
‡Marioff, Inc., Linthicum, MD

14. ABSTRACT

The effects water mist has on the overpressures produced by the detonation of 50 lb equivalent of high explosives (HE) TNT, Destex, and PBXN-109 in a chamber is reported. The overpressures for each charge density were measured with and without mist preemptively sprayed into the space. The impulse, initial blast wave, and quasi-static overpressure measured in the blast mitigation experiments were reduced by as much as (40%, 36%, and 35%) for 50 lbs TNT, (43%, 25%, and 33%) for 50 lbs TNT equivalent Destex, and (49%, 39%, and 41%) for 50 lbs TNT equivalent PBXN-109 when water mist was sprayed 60 seconds prior to detonation at a concentration of 70 g/m^3 and droplet Sauter Mean Diameter (SMD) of 54 μm. These results suggest that current water mist technology is a potentially promising concept for the mitigation of overpressure effects produced from the detonation of high explosives.

15. SUBJECT TERMS

Water mist	Destex	Overpressure
TNT	PBXN-109	

16. SECURITY CLASSIFICATION OF:

a. REPORT	b. ABSTRACT	c. THIS PAGE
Unclassified	Unclassified	Unclassified

17. LIMITATION OF ABSTRACT

UL

18. NUMBER OF PAGES

28

19a. NAME OF RESPONSIBLE PERSON
Heather D. Willauer

19b. TELEPHONE NUMBER (include area code)
(202) 767-2673

CONTENTS

BLAST MITIGATION USING WATER MIST: TEST SERIES II

1.0   BACKGROUND

The Navy's recognition of the benefits of water for fire suppression has led to the implementation of mist systems aboard ships [1-3]. There are modeling data that show the ability of mist to reduce overpressure and therefore limit shipboard damage caused by an explosion from a combat or terrorist attack [4-6]. Water mist, water-walls, and active and passive water deluge systems as a blast mitigating techniques have proven to be quite effective in reducing the effects caused by condensed-phase explosions and vapor-cloud explosions [7-10]. The mechanism by which mitigation has been achieved in these scenarios is dependent on several parameters. These parameters include the water mist density (the droplet size distribution and its concentration), the geometric complexity of the area being mitigated, and the chemical composition of the explosive (missile, TNT, dust cloud) [8,11]. Such parameters and their effects on mitigating explosions have not been well quantified, thus the design and implementation of these systems for mitigating specific events such as a shipboard explosion has been limited.

Ideally a shipboard water mist system would mitigate initial blast overpressures and any quasi-static overpressures and secondary effects caused by a blast. A shipboard environment is quite complex having several different levels of confined compartments that contain varying degrees of congestion. Studies indicate an explosion, in such an environment, would create reflecting shock waves that could cause additional increases in overpressures, thus causing even further damage to the ship [12]. The other concern is the amount of time and water mist needed to effectively achieve blast mitigation in the event of an attack [13].

In order to begin to address these issues the Naval Research Laboratory (NRL) conducted a series of blast mitigation tests sponsored by the Office of Naval Research in the summer of 2005. The tests were carried out in a bombproof chamber located at the Naval Surface Warfare Center (NSWC) Indian Head, Maryland. The objective of the studies was to utilize lower charge density explosions of 0.9 kg, 2.2 kg, and 3.2 kg (2 lbs, 5 lbs, and 7 lbs) TNT to establish the ability of water mist to mitigate the overpressures associated with detonations in a confined space. The studies showed that quasi-static overpressures were reduced by as much as 47%, and both the start of the initial blast overpressure and quasi-static pressures were delayed [13]. The water mist characterization studies indicated that mitigation was achieved with droplet sizes ranging from 35 - 550 μm with a Sauter Mean Diameter (SMD) greater than 50 μm [14]. SMD is the diameter of the droplet whose surface to volume ratio is equal to that of the entire spray [15].

2.0   OBJECTIVE

The Blast Mitigation Test Series 2 involved higher charge density detonations of different high explosives (HE) for the purpose of scaling and identifying the critical water mist parameters responsible for the mitigation of overpressures and secondary effects associated with blasts.

The tests series had 4 primary objectives:

_____

- To investigate the ability of water mist to mitigate larger-scale explosions using 23 kg (50 lbs) of TNT (or equivalent).
- To determine and predict mitigation properties of the water mist by measuring and quantifying blast mitigation overpressures as a function of water mist parameters.
- To investigate water mist mitigation of explosives having different chemical compositions.
- To utilize theoretical models to guide and interpret experiments.

3.0   APPROACH

This test series was broken into three phases. Phase I, the water mist system was installed in the overhead of the chamber, and characterized to achieve a series of water mist differing in droplet size and water mist concentration. Phase II, the water mist compositions were used to investigate their mitigating effects on three different HE detonations. Phase III involved collecting the initial blast overpressures generated by the three different HE detonations. In this phase no water mist was introduced into the chamber.

4.0   TEST DESCRIPTION

4.1   Test Chamber
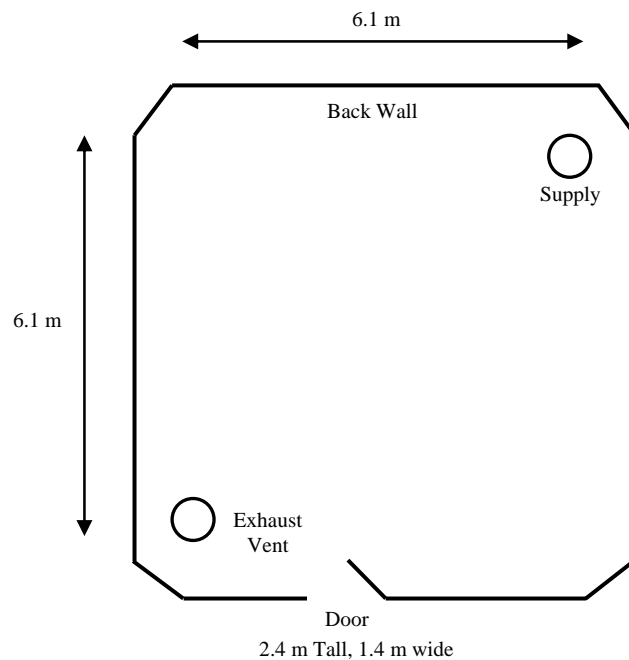

Figure 1. Schematic of the chamber showing the inside dimensions and locations of the ventilation piping.

This test series was conducted in a bombproof chamber located at the Naval Surface Warfare Center (NSWC), Indian Head, Maryland. The size and magnitude of the charges detonated specified the chamber size and dimensions used for the test series. The previous test series

utilized a chamber whose volume was 4.6 m x 4.6 m x 3.1 m (15.1 ft x 15.1 ft x 10.1) [13]. That chamber was rated for overpressures associated with 4.5 kg (10 lbs) detonations of TNT. In the present test series, the chamber volume was 6.1 m x 6.1 m x 4.9 m (20 ft x 20 ft x 16 ft) and it accommodated overpressures equivalent to 23 kg (50 lbs) of TNT. Both chambers are composed of reinforced concrete lined with steel plate. Figure 1 is a schematic of the inner dimensions and locations of the door and ventilation system of the chamber used in the test series.

The ventilation system consisted of an exhaust pipe and supply pipe that protruded 0.91 m (0.33 m OD, 0.30 m ID) ((3 ft (13" OD, 12" ID)) down from the overhead into the chamber. The supply pipe had a manually controlled fan used to circulate air into the chamber following an experiment, and the exhaust pipe vented to the open atmosphere. The vent pipe remained open to the atmosphere at all times. All the explosive charges utilized in this test series were supplied by NSWC Indian Head, and each charge was detonated in the center of the chamber. The bottom of the charge was 1.5 m (5 ft) above the deck and was directed down.

4.2   Phase I: Water Mist System and Characterization

In Phase I, the overhead of the chamber was outfitted with the water mist system as shown in Figure 2. This consisted of assembling the stainless steel piping and installing the water mist nozzles. As shown in Figure 2, the water mist system had nine available nozzle positions and the positions were spaced approximately 1.5 meters apart.
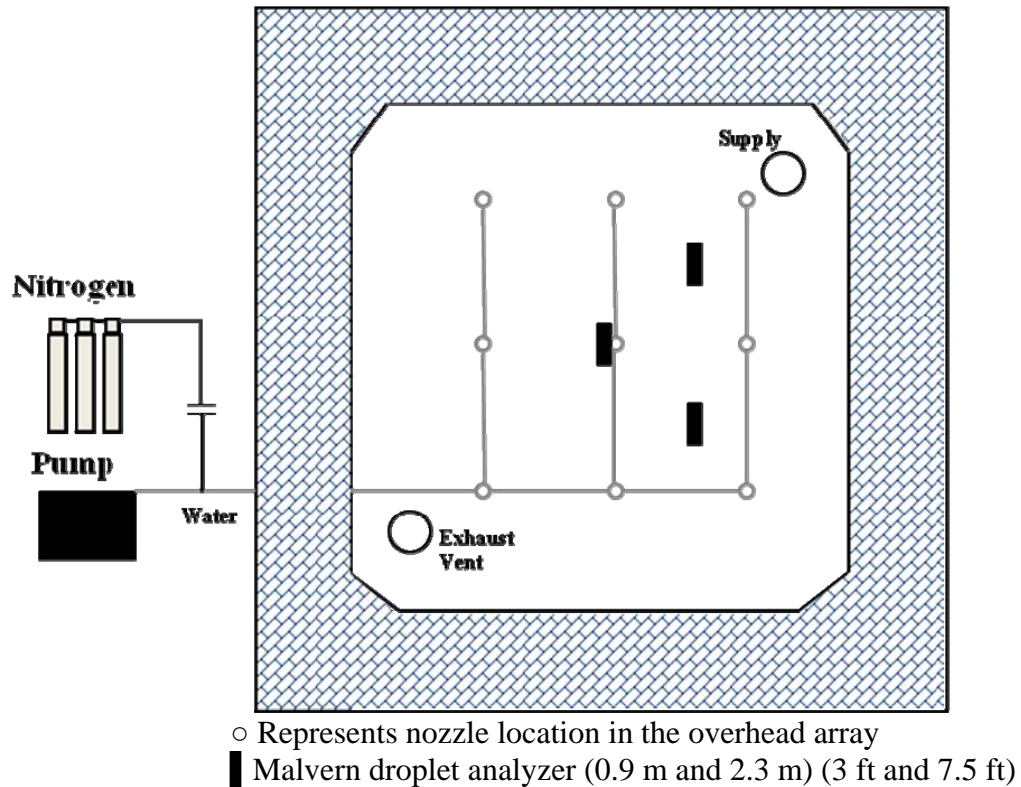

○ Represents nozzle location in the overhead array
▌Malvern droplet analyzer (0.9 m and 2.3 m) (3 ft and 7.5 ft)

Figure 2. Schematic of water mist system in the overhead of the chamber

3

For this test series, the water mist system was specifically designed and configured to provide more flexibility and control over the water mist generated in the chamber. A hybrid water mist option and a series of different nozzle sets (shown in Table 1) were used to achieve a range of different droplet size and water mist concentrations (shown in Table 2). The hybrid water mist was created with the addition of nitrogen to the water mist system as shown in Figure 2. The water mist system became a dual flow system where both nitrogen and water exited the nozzles simultaneously. The nitrogen flow enhanced droplet break-up as they exit the nozzles. Because of the system flexibility, the introduction of nitrogen into the water mist system was easily incorporated.

Table 1. Nozzle Set

Nozzle Set	Manufacturer	Nozzle Model Number	K factor	Flow
1	Marioff	4S 1MC 8MB 1000	1.9 lpm/bar^0.5	19 lpm at 100 bar
2	Marioff	4S 1MB 6MB 1000	1.4 lpm/bar^0.5	14 lpm at 100 bar
3	Marioff	3N 1MA 4MA 1000	0.5 lpm/bar^0.5	5 lpm at 100 bar

Table 2. Water Mist Properties

Nozzle Set	Pressure	Water Mist Flow Rate	Con	Dv(10)	Dv(50)	Dv(90)	SMD
1	100 bar	171 lpm	70 g/m^3	52 μm	165 μm	332 μm	54 μm
1	35 bar	101 lpm	57 g/m^3	71 μm	184 μm	335 μm	105 μm
1	100 bar	Hybrid	36 g/m^3	13 μm	80 μm	224 μm	27 μm
2	100 bar	126 lpm	60 g/m^3	6 μm	147 μm	337 μm	30 μm
2	35 bar	74 lpm	47 g/m^3	68 μm	205 μm	363 μm	116 μm
3	100 bar	95 lpm	29 g/m^3	64 μm	175 μm	333 μm	83 μm

In these tests positive displacement electric driven pumps were used rather than a pressurized nitrogen system as in the previous test series to push the water through the nozzles and into the chamber [16]. The pump provides the capability of delivering water at a constant flow and pressure (maximum 194 lpm at 120 bars). As a result, a steady state water mist composition inside the chamber was achieved and maintained, unlike the previous test series [13,14]. Figure 3 shows the pump configuration (please note only two of the pumps were required for these tests) and Table 3 provides the pump motor specifications and capacity.

Figure 3. The pump and reservoir assembly

Table 3. Pump Specifications

Motor	Power	Supply	Flow
Motor 1	27 kWatts (36 HP)	480 Vac, 3-Phase, (50 Amps)	97 lpm at 140 bar
Motor 2	22 kWatts (30 HP)	480 Vac, 3-Phase, (46 Amps)	97 lpm at 120 bar
Together	49 kWatts (66 HP)	480 Vac, 3-Phase, (100 Amps)	194 lpm at 120 bar

A state-of-the-art laser light scattering analyzer (Malvern Spraytec Malvern Instruments Inc., Southborough, MA) was placed inside the chamber to determine the critical point at which the mist concentration and droplet size distribution, for a given nozzle configuration, reached a steady state. These properties were measured for different nozzle configurations used to mitigate the HE blasts in Phase II of the test series. Table 2 provides the water mist concentrations and droplets sizes that the test series achieved. In addition, the Table indicates the nozzle set used to create the mist. The nozzle set properties are provided in Table 1.

4.3   Phase II: Explosion Tests

Phase II involved seven separate detonations experiments. Four of these experiments were conducted with 23 kg (50 lbs) of TNT while two were conducted with 50 lbs TNT equivalent

PBXN-109, and the final detonation was with 50 lbs TNT equivalent Destex. For each 50 lb TNT detonation experiment, one of the well characterized water mist compositions shown in Table 2 was used to mitigate the overpressures associated with the detonation. By comparing the mitigating efficiencies of the water mist systems utilizing TNT, emphasis was placed on the function each mist parameter had in the mitigation process. For a defined set of mist conditions, the blast was detonated in the chamber after the mist had reached steady state.

The water mist composition that was most effective in the blast mitigation of 50 lbs of TNT was used to mitigate the overpressures associated with two different 50 lb TNT equivalent aluminized HE charges (Destex and PBXN-109). Emphasis was placed on comparing and determining the mitigating efficiency of the water mist on explosives whose chemical composition and reaction process were different than that of TNT.

4.3.1 TNT

TNT (2,4,6 Trinitrotoluene) is a solid secondary high explosive currently used in military weapons and civilian mining processes. Secondary explosives simply require a primary or initiating explosive to ignite it [17]. This material was chosen for this test series because it is one of the most common and well understood explosives, and small-scale explosions of TNT (0.9 kg, 2.2 kg, and 3.2 kg) (2 lbs, 5 lbs, and 7 lbs) have demonstrated the ability of water mist to effectively suppress the overpressures associated with the detonation of this type material [13].

Two of the most important detonation performance parameters that represent the effectiveness of different explosives are the detonation velocity and detonation pressure (Chapman-Jouguet, C-J) [11,18,19]. Detonation velocity is the speed at which the detonation wave travels through the explosive [17,18]. Both parameters are dependent on the material's heat of detonation, charge density, and composition [11,18,19]. Table 4 shows the performance parameters for TNT and how they compare to other TNT and RDX based explosives. Equation 1 provides a simple reaction mechanism for TNT [5,18].

$$C_7H_5N_3O_6 \rightarrow 2.5\ H_2O + 3.5\ C_{(s)} + 3.5\ CO + 1.5\ N_2 + 247\ kcal/mol\ TNT \quad (1)$$

Table 4. Explosive Performance Parameters

Material	Density (g/cm^3)	Detonation Velocity (fps)	Detonation (C-J) Pressure (GPA)	Heat of Detonation ΔH^o_d (kcal/mole)
TNT	1.65 [18]	23,000 [18]	20 [18,11]	247 [5,18]
TNT/Al (89.4/10.6)	1.72 [11]	23,000 [11]	21*	
TNT/Al (78.3/21.7)	1.8 [11]	23.000 [11]	22*	
TNT/Al (67.8/32.2)	1.89 [11]	23,000 [11]	23*	
RDX	1.81 [18]	29,000 [18]	35*	335.4 [18]
RDX/Al (90/10)	1.68 [11]	26,000 [11]	27*	
RDX/Al (80/20)	1.73 [11]	25,000 [11]	26*	
RDX/Al (70/30)	1.79 [11]	25,000 [11]	26*	

*Detonation Pressures calculated using reference [16].

From Table 4 and the reaction mechanism, TNT is notably oxygen deficient, less dense, and its decomposition reaction produces less energy than other energetic materials. This yields lower C-J pressures and slower detonation velocities [5,18,19].

4.3.2   Destex

Destex is desensitized Tritonal that was developed in the 1970's [16]. The explosive is TNT based and contains approximately 74.4% TNT, 19.1% Aluminum powder, 1.9% carbon black. This compound is used by the US Navy and Air Force in a missile designed to sink warships in the open ocean. The missile, AGM-84 Harpoon SLAM [Stand-Off Land Attack Missile] contains 98 kg (215 lbs) of Destex and is the only missile used by the US military with anti-ship warfare as the primary objective [17].

Aluminized composite explosives are classified as having nonideal behavior [11,20]. In such materials, the metal additive reacts with the detonation products expanding behind the detonation zone [11,20]. This causes an increase in temperatures and pressures associated with the blast. Table 4 shows how the detonation pressures and charge densities of TNT/Al composites increase as the percentage of aluminum increases. As a result, the addition of aluminum powder has traditionally been used in military applications to enhance air blasts effects, increase bubble energies in underwater weapons, raise temperatures, and create incendiary effects [11].

4.3.3   PBXN-109

PBXN-109 is composed of 64% RDX, 20% Al, and 7.4% polymer based binder. This explosive was selected for this test series because its blast mechanism and performance parameters (Table 4) are significantly different than explosives primarily composed of TNT. RDX (hexahydro-1,3,5- trinitro- 1,3,5- triazine) is a cyclic amine that is used in several different military explosives such as HBX, H-6, Cyclotol, and Compositions A, B, and C [17]. RDX is second to nitroglycerin in strength among common explosives, and it is considered the most powerful and brisant of the military high explosives [17]. Equation 2 gives a simple reaction mechanism for RDX [18].

$$C_3H_6N_6O_6 \rightarrow 3\ H_2O + 3\ CO + 3\ N_2 + 335.4\ \text{kcal/mol RDX} \qquad (2)$$
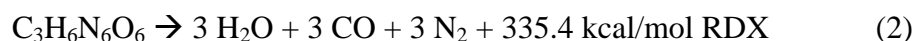
From Table 4 and the reaction mechanism, RDX is denser, has a greater balance of oxygen, and its decomposition reaction produces more energy (335.4 kcal/mol) than the TNT based explosives. This yields higher C-J pressures and faster detonation velocities [18]. Table 4 also shows that the addition of aluminum appears to lower the performance parameters of RDX. Despite the slight reduction, the values are still greater than those for TNT.

4.4   Phase III: Base Line Explosion Tests

In Phase III, the initial blast overpressures and quasi-static overpressures were measured for the three different HE charges (TNT, Destex, and PBXN-109) used in Phase II. These initial tests provided baseline measurements for comparing and determining the mitigating efficiency of water mist as a function of water mist characteristics and chemical blast mechanisms, when it is introduced into the chamber during Phase II.

5.0   TEST MATRIX

5.1   Water Mist Test

Twenty three tests were conducted in Phase I to achieve and characterize the mist compositions listed in Table 2. The mist characteristics measured at the location of the charge were deemed the most relevant to this analysis.

5.2   Explosion Test Matrix

The explosion test matrix is provided in Table 5.

Table 5. Explosion Test Matrix

| Test	Charge	Test Type	Water Mist System Flow Rate	Water Mist Droplet Concentration	Droplet Mean Diameter
1	TNT	Water mist	95 lpm	29 g/m^3	176 µm
2	TNT	Water mist	101 lpm	57 g/m^3	184 µm
3	TNT	Water mist	Hybrid water mist	36 g/m^3	80 µm
4	TNT	Water mist	171 lpm	70 g/m^3	165 µm
5	PBXN-109	Water mist	171 lpm	70 g/m^3	165 µm
6	Destex	Water mist	171 lpm	70 g/m^3	165 µm
7	PBXN-109	Water mist	95 lpm	29 g/m^3	175 µm
8	Destex	Baseline			
9	PBXN-109	Baseline			
10	TNT	Baseline			

6.0   INSTRUMENTATION

The water mist properties and the initial blast overpressures and quasi-static overpressures generated by the blast were of the most interest in this test series.

6.1   Explosion Instrumentation

6.1.1   Data Acquisition System

The primary data acquisition system used in the explosion phases of the test series was supplied by NSWC Indian Head. The system was primarily used to collect and process the overpressure data measured by the pressure transducers. The data acquisition system used was a National Instruments PXI system capable of collecting 2.5 million samples per second using a PXI-6133 card. To give 5 seconds worth of data, 100,000 samples per second was chosen.
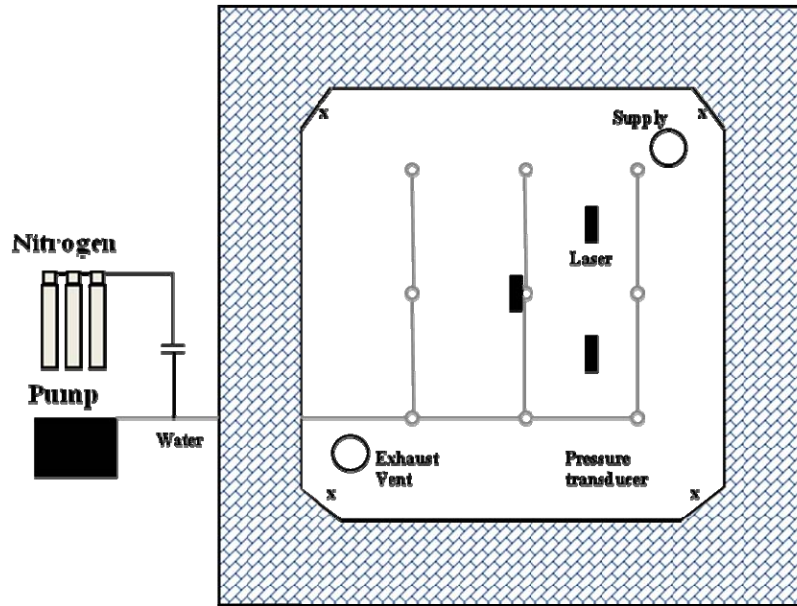
x Pressure transducers 2 m (6.5 ft) off chamber floor

▌ Malvern droplet analyzer (0.9 m and 2.3 m) (3 ft and 7.5 ft)

Figure 4. Instrument Location in Chamber

6.1.2   Pressure Transducers

The chamber was outfitted with pressure transducer boxes in each corner approximately 6.5 feet off the deck as shown in Figure 4. Any number of transducers can be mounted in these boxes given the test's criteria. For this test series, one box was outfitted with one Kulite KTE-190-1000A transducer and the other three gauges were Endevco 8530B-500. The gauges have a maximum pressure range of 200 psi and they were flush mounted in the boxes. A thin layer of grease was placed in front of each gauge to protect them from heat and blast effects.

All gauges were calibrated at the start and end of each test series or if the output appeared questionable. Pressure data were recorded at 100,000 samples per second for a minimum duration of 5 seconds. The data were recorded using at a 100 kHz low pass filter setting, which could have been digitally filtered later if necessary.

6.1.3   High Speed Video

A high speed video camera was provided by NSWC Indian Head to capture the explosion event in the chamber (the fire ball) with and without water mist. The following camera was used:

- Vision Research Phantom 4s – capable of 3100 frames per second at a resolution of 800x600. Frame rate increases with scaled down resolution.

Further information on the camera can be found at www.visiblesolutions.com.

9

6.2   Water Mist Characterization

6.2.1   Droplet Size Analyzer

Each configuration of the water mist system was characterized by a droplet size analyzer (Malvern Spraytec Malvern Instruments Inc., Southborough, MA). The analyzer provided water droplet size distribution and mass loading measurements as a function of time. The Sauter Mean Diameter (SMD) is primarily used to quantify droplet size distribution of the spray, however the instrument provides other critical spray composition parameters such as Dv(10), Dv(50), and Dv(90). Dv(10) represents the drop diameter below which 10% of the total liquid volume of the material exits. Dv(50) is the mass median droplet size, and Dv(90) is the drop diameter below which 90% of the total liquid volume of material exists [15]. The analyzer was configured with the following options: 200 mm focal length lens, 10 mm laser beam diameter, and continuous mode operation. The 200 mm focal length lens is capable of measuring droplet sizes between 1 - 400 µm. The Malvern was used to map the concentration and droplet size in the chamber at three separate locations shown in Figure 4, and two different heights (0.9 m and 2.3 m) (3 ft and 7.5 ft) at those locations. These measurements will be used in conjunction with the optical density meters to provide mist concentration measurements.

7.0   SAFETY

Safety was paramount in all field tests involving explosive operations. All personnel handling explosives followed approved Hazard Analysis and referenced Standard Operating Procedures (SOP) prepared by and approved by Indian Head personnel. Test operations were under the control of Indian Head personnel.

8.0   RESULTS AND DISCUSSION

8.1   Water Mist Characterization

Prior to the detonation experiments, the average droplet properties were measured for the mist produced by a series of different nozzle sets shown in Table 1. The measurements were made at the charge location. Mist droplet size and concentration are key parameters in determining the time scales for which droplet breakup, momentum transfer, evaporation, and radiation absorption could extract energy from the shock front and suppress overpressure created from a blast [21]. Thus the objective of this test series was to achieve a range of different mist concentrations and droplet sizes, using the nozzle sets given in Table 1, to determine the how each mist parameter affected the blast mitigation process. Table 2 shows the average water mist properties produced over a sixty second spray interval by the 3 nozzle sets shown in Table 1 operating under different settings and conditions (reduction in pressure and additions of nitrogen).

Detonations were initiated after mist was preemptively sprayed into the chamber for sixty seconds in the HE detonation experiments with water mist. Sixty seconds was chosen to provide sufficient time to initiate the mist system and secure the blast test area before detonation for safety reasons.

As shown in Figures 2 and 4 the mist was sprayed from the overhead of the chamber using a nine nozzle array. The mist contains different size droplets, which settle to the floor at different rates due to air resistance. Table 2 shows the nozzle set with the highest K factor (4S 1MC 8MB 1000) produced the highest measured mist concentration (70 g/m^3) in the chamber with a droplet SMD of 54 µm. When the pressure was reduced from 100 bar to 35 bar for that nozzle set and conditions, the mist flow rate and mist concentration in the chamber were reduced from 171 lpm to 101 lpm and 70 g/m^3 to 57 g/m^3. This reduction in pressure at the nozzles also caused the droplet size to increase as shown by an increase in SMD from 54 µm to 105 µm and Dv(10) from 52 µm to 71 µm. With the addition of nitrogen to the system, it became a dual flow hybrid system that caused further reductions in mist concentration to 36 g/m^3 and droplet size SMD to 27 µm. The dual flow conditions reduced the amount of water exiting the nozzles and the nitrogen enhanced droplet break-up as they exited the nozzles. These mist conditions created the least amount of observable residual water on the chamber floor and walls.

The nozzle set with the second largest K factor (4S 1MB 6MB 1000) operating at 100 bar produced similar mist concentrations achieved by the first nozzle set operating at a reduced pressure of 35 bar. Though the concentrations were similar, the second set of nozzles produced significantly smaller droplets as indicated by a reduction in SMD to 30 µm and Dv(10) to 6 µm. As expected, when the pressure at the nozzles was reduced from 100 bar to 35 bar the droplet size increased as shown by an increase in SMD from 30 µm to 116 µm and Dv(10) from 6 µm to 68 µm and the droplet concentration measured was reduced from 60 g/m^3 um to 47 g/m^3. The final set of nozzles characterized (3N 1MA 4MA 1000) produced similar mist concentrations (29 g/m^3) to the hybrid set of conditions (36 g/m^3) with significantly different droplet characteristics.

The differences in droplet size distribution under hybrid conditions and the conditions produced using the 3N 1MA 4MA 1000 nozzle set is shown in Figure 5. The size distribution results were averaged over a 60 second spray period and the fraction of smaller droplets produced under the hybrid conditions over this period was a factor of 3 to 5 times greater than those produced by the 3N 1MA 4MA 1000 nozzle set as indicated by the reduction in SMD and Dv(10). Since the total evaporation rate of the mist depends linearly on the mass concentration of water and on the inverse square of the droplet diameter, the shift to smaller droplets produced under hybrid conditions would indicate the evaporation rate of the mist was greater [15]. The difference in droplet characteristics for nozzle sets producing similar concentrations enabled a parametric set of droplet conditions to be achieved for investigating the effects droplet concentrations and sizes have on mitigating the blast.

Figure 6 shows the droplet size distribution for the nozzle set and conditions that produced the largest measured mist concentration in the chamber. In the Figure Dv(10), Dv(50), and Dv(90) are 52 µm, 165 µm, 332 µm. These values are comparable to those values measured for the mist system used in the 7 lb TNT detonation experiments Dv(10) 51 µm , Dv(50) 171 µm, and Dv(90) 356 µm conducted at Indian Head, and the details of the mist system and chamber dimensions for those tests are available [13]. The values for Dv(10), Dv(50), Dv(90), and SMD for both test series represent the characteristics of the mist before it is affected by the incoming shock wave. Once the shock front has passed, these values will be subjected to heat and shear forces generated behind the shock front [21,22].
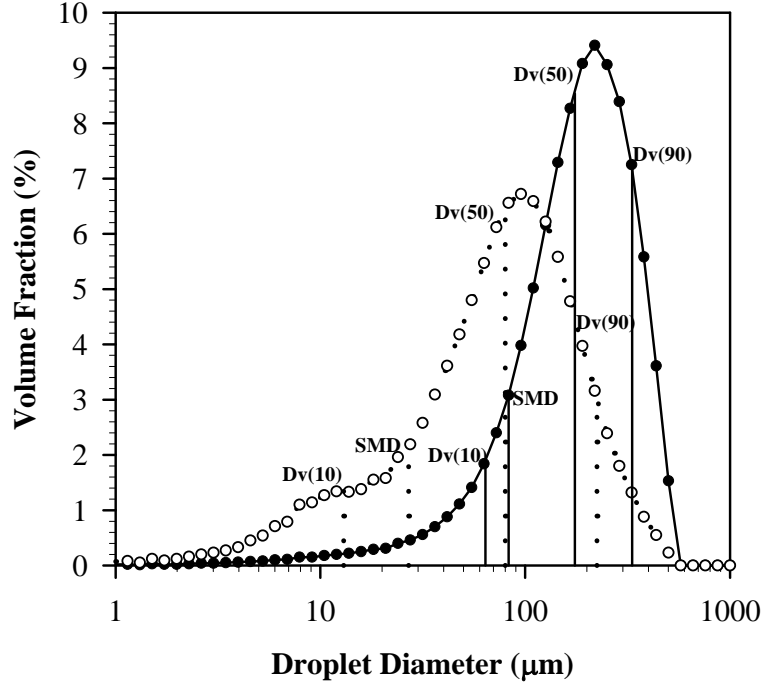
Figure 5. Water mist droplet size distribution measured over a 60 second spray period for nozzle set 1 (-○- 4S 1MC 8MB 1000, 100 bar, hybrid) SMD, Dv(10), Dv(50), Dv(90) [27 μm, 13 μm, 80 μm, 224 μm] and nozzle set 3 (-●- 3N 1MA 4MA 1000, 100 bar) SMD, Dv(10), Dv(50), Dv(90) [83 μm, 64 μm, 175 μm, 333 μm].
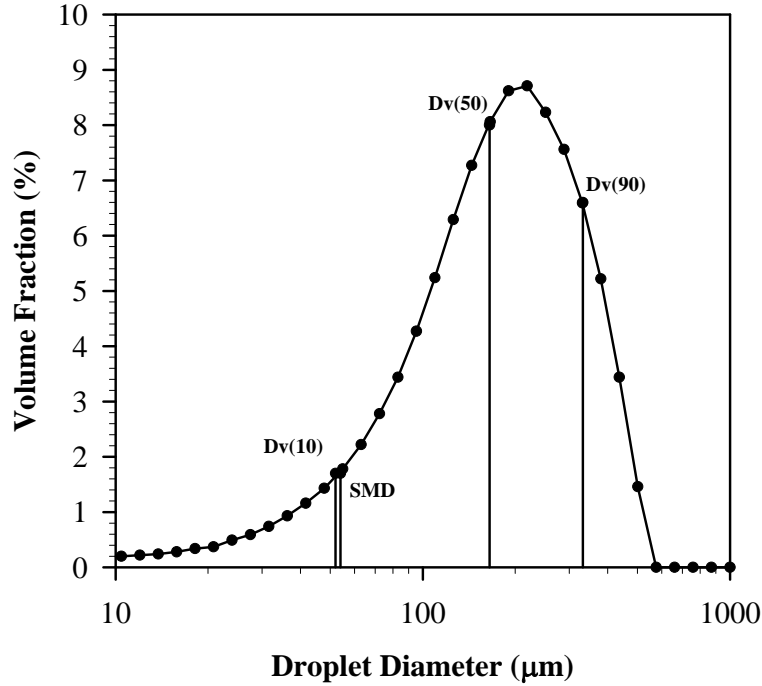

Figure 6. Water mist droplet size distribution measured over a 60 second spray period for nozzle 1 (4S 1MC 8MB 1000 operating at 100 bar). SMD, Dv(10), Dv(50), Dv(90) [54 μm, 52 μm, 165 μm, 332 μm].

Since the total evaporation rate of the mist could play a significant role within the short time scales of an explosion, a key objective in this test series was to produce and maintain steady state water mist conditions inside the chamber. Figure 7 compares the mass concentration of water as a function of time for mist conditions produced by different nozzle sets shown in Table 1 operating under different settings and conditions shown in Table 2. The nozzle set (4S 1MC 8MB 1000) that produced the highest measured mist concentration (70 g/m^3) in the chamber fluctuates during the 60 second spray interval. However, when averaged over 20, 60, and 90 seconds the average mist concentrations were 70 ± 10 g/m^3. The nozzle sets and operating conditions that produced the least amount of water in the chamber (hybrid and 3N 1MA 4MA 1000) created more stable concentration profiles. Thus the dynamics of the mist produced are such that less turbulence and mixing takes place as less water is pumped into the chamber. The Figure also shows the mist concentration for each different set of mist conditions reaches its average steady state output within seconds of initiating the pump, indicating no need for long preemptive spray intervals. This is critical because in the event of a threat, an area may be secured with water mist within seconds to reduce blast effects.
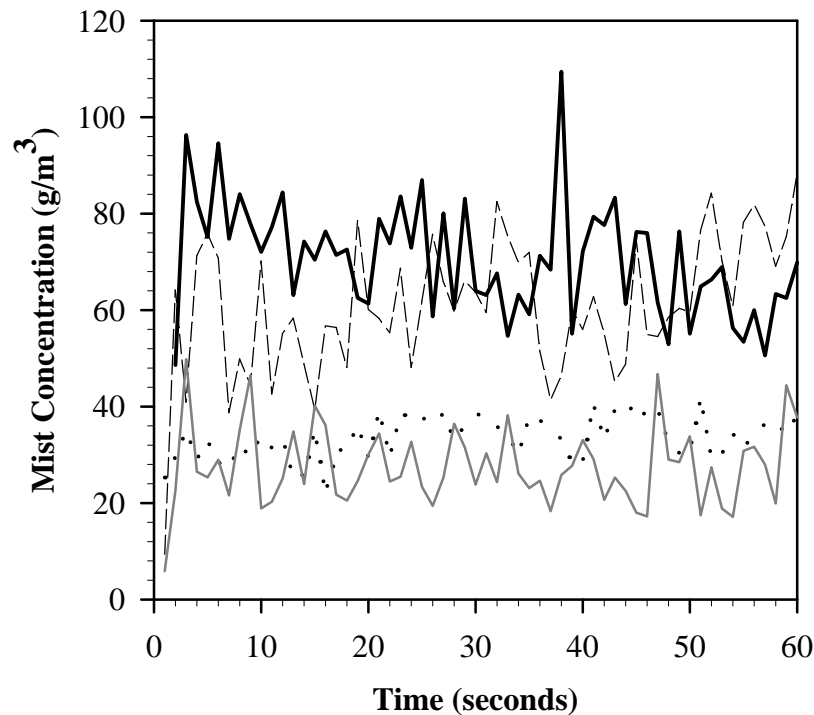

Figure 7. Mass Concentration of water as a function of time for mist conditions shown in Table 3: (black line —) Nozzle set 1 (100 bar); (- -) Nozzle set 1 (35 bar); (…) Nozzle set 1 (Hybrid); (gray line —) Nozzle set 3 (100 bar).

It is estimated that approximately 171 liters of water was sprayed into the chamber in 60 seconds to achieve the highest mist density measured in the chamber for this test series. If the water was completely suspended in the air, the average droplet concentration would be 938 g/m^3. This value is over twice the 412 g/m^3 that would have been theoretically achievable in the 7 lb small scale detonation experiments. The actual measured values for these mist systems were 70 g/m^3

(shown in Table 2) and 87 g/m^3. Thus only about 7.5% of the 938 g/m^3 and 21% of the 412 g/m^3 were suspended at any given time in the different test series. In addition only 6 to 12% of the mist generated from each of the other mist conditions used in this test series was found to be suspended in the air. This is likely the results of droplets settling to the floor and along the chamber walls. Thus continued spraying of water mist beyond the settling time might not have contributed to the mist concentration in the air.

The droplet concentration values shown in Table A-1 of Appendix A for two different heights at the charge location are found to be higher than those values closer to the chamber wall. In the blast experiments with water mist, the bottoms of the explosives were placed approximately 1.5 m above the chamber floor.

The total evaporation rate of the mist will largely depend on the mass concentration and inverse square of the droplet diameter. How it plays a role in the short time scales of an explosion is critical to determining the mechanisms behind explosion suppression by water mist. Therefore the evaporation time scales associated with the droplet properties of the mist injected into the chamber are evaluated using the d^2-law shown in Equation 3 as [15]:

$$d_o{}^2 = \lambda t_{ev} \tag{3}$$

where d_o is the initial droplet diameter before the explosion (SMD) and t_{ev} is the time for complete droplet evaporation.

The evaporation constant λ is given in Equation 4 as:

$$\lambda = 8\, k_g \ln(1 + B)/Cp_s\rho_w \tag{4}$$

where k_g is the thermal conductivity of air, Cp_s is the specific heat capacity of air at 673 K and ρ_w is the density of water. The heat transfer number B is shown in Equation 5 as:

$$B = Cp_s\, (T_\alpha - T_s)/L \tag{5}$$

where L is the latent heat of water vaporization, T_α is 673 K and T_s is the water surface temperature corresponding to water vaporization, 373 K. T_α was chosen based on the simulations performed by Ananth that suggest the water droplets encounter temperatures between 600 and 700 K behind the shock front at 2 milliseconds [22]. Figure 8 shows the time in which it takes for droplets having diameters between 5 and 400 μm to evaporate without breaking up. Equation 3 shows that at these temperatures in ambient air, a 5 μm droplet will evaporate within 2 milliseconds, a 51 μm droplet will evaporate within 60 milliseconds, and 400 μm droplet will evaporate within 3 seconds. The effect of high gas velocities generated from the explosion will shear the droplets causing breakup which will significantly lower the evaporation time scales.
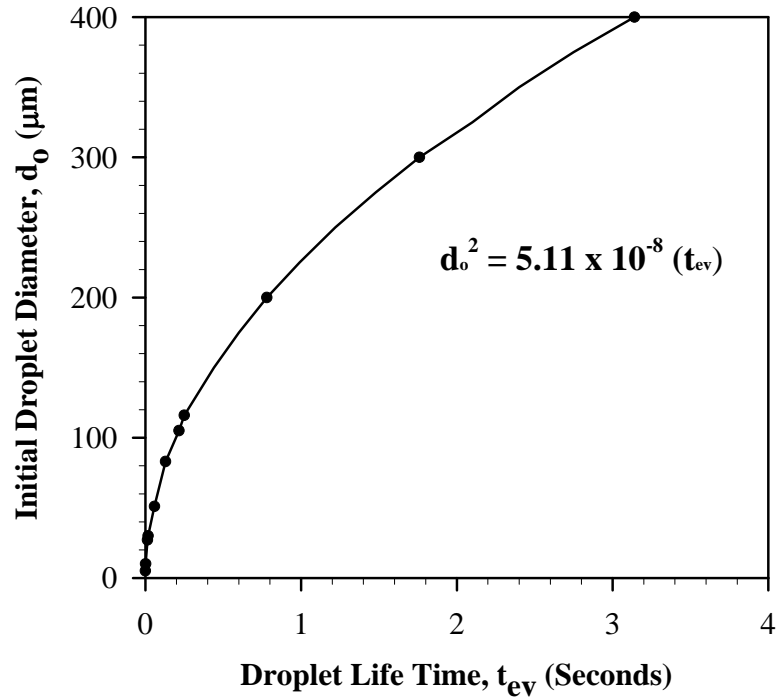
14

Figure 8. Initial droplet size (5 - 400 μm) as a function of time for complete evaporation**.**

8.2 Effects of Mist on Blast

Figure 9, 10, and 11 show the pressure pulse generated from the detonation of 50 lb TNT, 50 lb TNT equivalent Destex, and 50 lb TNT equivalent PBXN-109 with (grey) and without (black) water mist. TNT was chosen for this test series because it is one of the most common well characterized and understood explosives, and small scale explosions of TNT (0.9 kg, 2.2 kg, and 3.2 kg) (2 lbs, 5 lbs, and 7 lbs) in an enclosure have demonstrated the potential for mist to suppress explosion related effects [13]. The effect water mist has on suppressing overpressures generated by the detonation of explosives simulating traditional materials used in military application (Destex and PBXN-109) is also of interest [17].

Prior to the detonation in the mist experiments, water was sprayed into the chamber for a finite time period of 60 seconds. The mist was secured approximately 20 to 40 seconds after the detonation. In each detonation experiment the data acquisition system collected up to five seconds of data at 1×10^{-5} second intervals.
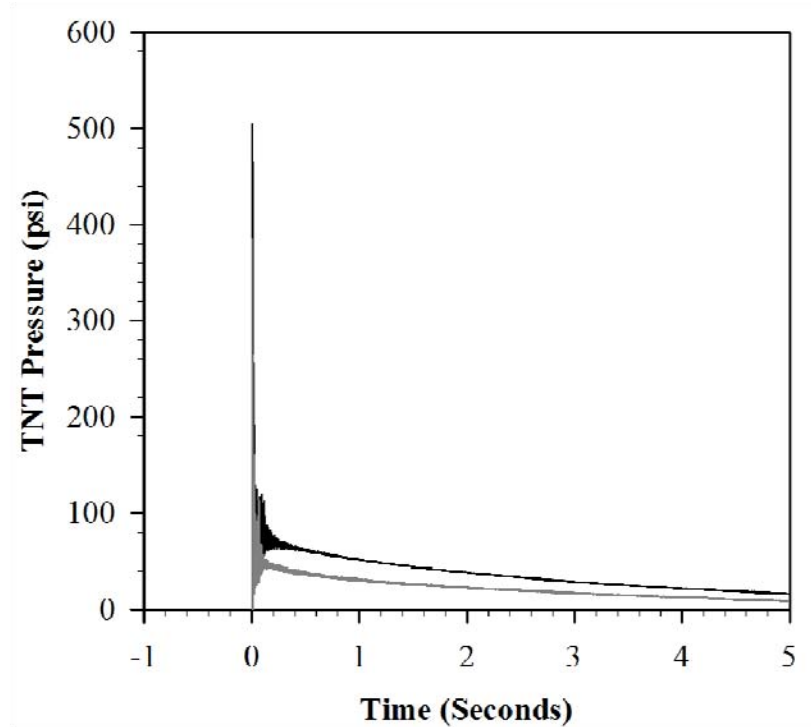
Figure 9. 50 lbs TNT Pressure Trace with and without water mist: Black (baseline), Grey (water mist).
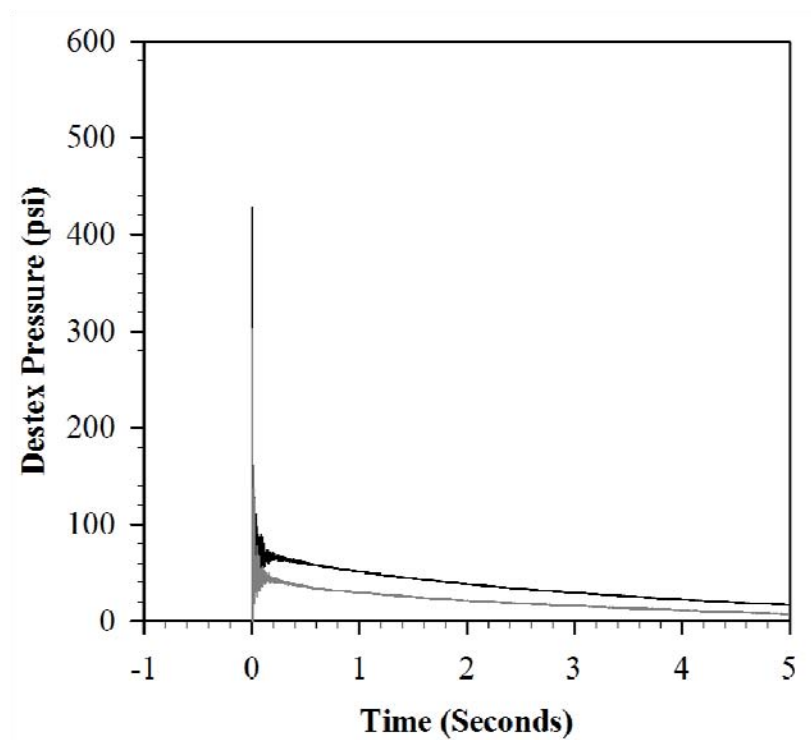

Figure 10. 50 lbs TNT equivalent Destex Pressure Trace with and without water mist: Black (baseline), Grey (water mist).
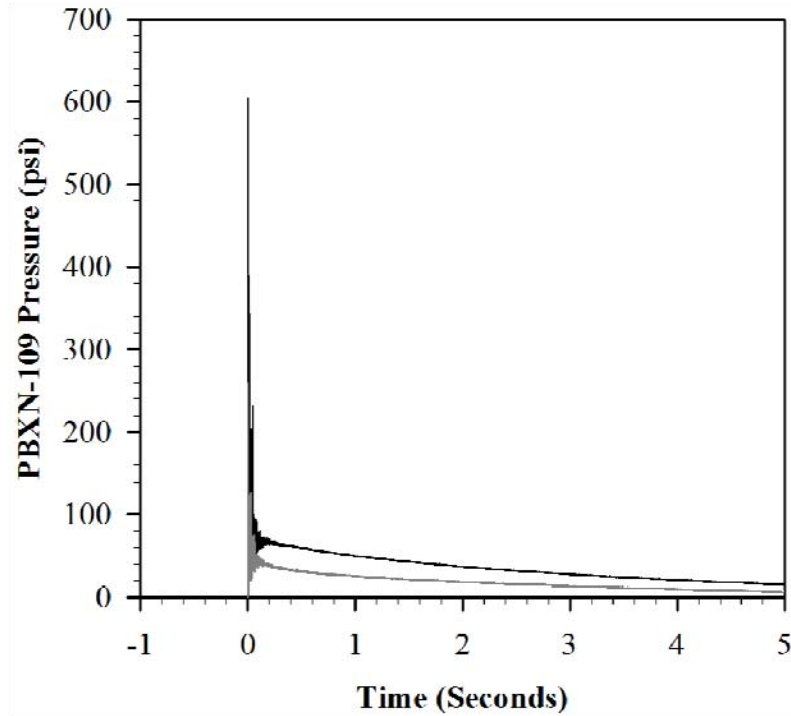
Figure 11. 50 lbs equivalents PBXN-109 Pressure Trace with and without water mist: Black (baseline), Grey (water mist).

In the detonation experiments shown in Figures 9, 10, and 11, the charges were detonated at time t=0. Upon detonation, the blast wave propagates across the air to the chamber walls. At the walls, the blast wave was reflected multiple times causing large fluctuations in the pressure trace. The amplitude of the fluctuation reached a steady value that decreased slowly with time because of gas venting out of the chamber and cooling of the explosive gases inside the chamber. From the pressure traces, the impulse and initial blast wave overpressure can be determined and compared. The impulse is defined by the area under the pressure trace from 0 to 5 seconds. The results are given in Tables 6 and 7.

In Table 6 the impulse and initial blast wave overpressures for different HE charges and different HE charge densities is higher without water mist. For different charge densities of TNT, the impulse and initial blast wave overpressures are the highest for 50 lbs TNT and the lowest for 7 lbs TNT with and without water mist [13]. Table 7 specifically shows the impulse and initial blast wave overpressures for 7 lbs TNT was suppressed by 44% and 43% compared to 40% and 36% suppression achieved using the highest mist density in the 50 lb TNT detonation experiments. Table 6 also indicates that the mist concentration measured in the chamber for the lower charge density detonation experiments was higher by 17 g/m^3. When the mist density is decreased from 70 g/m^3 to 57 g/m^3 in the 50 lb TNT detonation experiments, suppression of the impulse and initial blast is reduced from 40% and 36% to 26% and 16% (Table 7). Further reductions in mist concentration to 29 g/m^3 used in the PBXN-109 detonation experiments, show the impulse and initial blast suppressed by 9% and 16% compared to the 49% and 39% achieved using more water.

17

Table 6. Pressure Results

Charge Type	Mist Concentration (g/m³)	Droplet SMD (µm)	Impulse (psi*sec)	Initial Blast Wave (psi)	Quasi-static peak (psi)
7 lbs TNT	Baseline	0	39	184	35
7 lbs TNT	87	85	22	104	24
50 lbs TNT	Baseline	0	181	512	74
50 lbs TNT	70	54	108	327	48
50 lbs TNT	57	30	134	431	53
50 lbs TNT equivalent Destex	Baseline	0	179	430	70
50 lbs TNT equivalent Destex	70	54	102	324	47
50 lbs TNT equivalent PBXN-109	Baseline	0	175	449	71
50 lbs TNT equivalent PBXN-109	70	54	90	273	42
50 lbs TNT equivalent PBXN-109	29	83	159	375	57

Table 7. Suppression Results

Nozzle Set	Charge Type	Mist Concentration (g/m³)	Impulse (psi*sec)	Initial Blast Wave (psi)	Quasi-static peak (psi)
*	7 lbs TNT	87	44%	43%	31%
1	50 lbs TNT	70	40%	36%	35%
1	50 lbs TNT	57	26%	16%	28%
1	50 lbs TNT equivalent Destex	70	43%	25%	33%
1	50 lbs TNT equivalent PBXN-109	70	49%	39%	41%
3	50 lbs TNT equivalent PBXN-109	29	9%	16%	20%

*Nozzles and mist system described in reference [13].

The suppression results obtained for the aluminized explosives, Destex and PBXN-109 confirm thermodynamic and Navier-Stokes calculations that predicted the overpressure would be reduced in the presence of water mist [22]. This is significant because it was suggested that water mist in the chamber would lead to reactions between aluminum and water to form hydrogen. Thus these reactions would release energy and result in enhancing the blast overpressures instead of mitigating them. In addition, the suppression results indicate mist is effective in reducing overpressures associated with the detonations of materials having a different chemical composition (Destex and PBXN-109) than TNT.

In Figure 12 an arithmetic average was calculated to show the changes in overpressures as a function of time for the detonations of 50 lbs TNT and 7 lbs TNT with and without water mist in the chamber. A minimum time interval size of 1000 points (10^{-2} sec) was chosen to smooth the curve. Since the pressure is contained within the chamber, the smoothed overpressure curve shows how the pressure rises rapidly after the detonation to a maximum value before it decreases slowly with time as the explosive gases escape out the vent and cool within the chamber. The sustained pressure is called the quasi-static pressure. This pressure, not the initial blast wave, is believed to be responsible for damage within an enclosure [23]. The quasi-static peak pressure is measured from these smoothed curves by fitting a tangential line through the average peak pressure (0.2 sec – 0.5 sec) and extrapolating it back to the initial pressure rise [23].
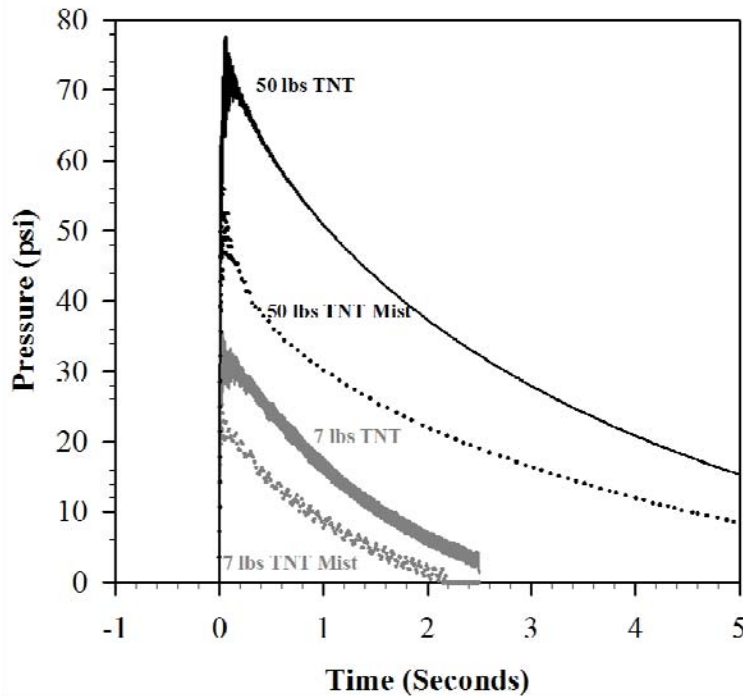

Figure 12. 50 lbs and 7 lbs TNT Smoothed Pressure Trace with and without water mist: 50 lbs TNT [Black, baseline (–), mist (·····)], 7 lbs TNT [Grey, baseline (–), water mist (·····)].

19

The results in Figure 12 and Table 6 highlight the significant change in overpressures measured for different charge densities of TNT with and without water mist. The quasi-static peak pressures are two times greater for the 50 lb detonations, and yet the suppression of the impulse, initial blast wave, and quasi-static peak pressures in Table 7 are comparable between the different charge densities. This strongly suggests that suppression is scalable to larger charge densities.

The quasi-static peak pressure reaches a maximum within 200 milliseconds in Figure 12. These time scales imply that mist droplets below 100 μm are well positioned to evaporate and extract energy from the blast (Equation 3). Thermodynamic calculations of droplet breakup energies performed by Adiga et al. suggest the droplet evaporation rate should increase as a result of the droplets fragmenting near the shock front [21]. While the energy from the breakup processes was found to be negligible, a significant increase in the surface area of the droplets should result in a tremendous increase in the droplet vaporization rate. In this case, a 200 μm droplet (0.78 seconds to evaporate, Equation 3) fragmented into 10 μm droplets (0.002 seconds to evaporate, Equation 3) would mean a 20 fold increase in droplet surface area and a 400 fold decrease in the time for the droplets to evaporate.

Recent simulations of a 50 lb detonation of high explosive in a 3.5 m radius spherical chamber performed by Ananth et al. indeed highlight the significance droplet breakup has on blast suppression [22]. The simulations show that a shock front propagates ahead of the thermal front immediately following the detonation. Thermodynamic and Navier-Stokes simulations performed with and without droplet breakup found that droplet breakup near the shock front enhanced the sensible and latent heat energy absorption by 100 times or more and cooled the gases in the region between the shock and thermal fronts. It was concluded from the simulations that the latent heat absorption by evaporation was the dominant mechanism by which water mist absorbed energy near the shock front.

Other simulations by Schwer and Kailasanath concluded that momentum absorption was the mechanism by which water mist suppressed the quasi-static pressures produced by small explosions of TNT (2 and 5 lbs) in an enclosure [24]. In these simulations droplets were not fragmented at the shock front so they were able to interact with the front as it was reflected multiple times. The droplet sizes (7-50 μm) and the mist concentrations (250-2000 g/m^3) used in the simulations far exceed the realistic size and quantities achievable with current technologies. For example, the highest mist concentration theoretically achievable in the 50 lb test series was 938 g/m^3 and 412 g/m^3 in the 7lb test series if all the water remained completely suspended in the air. However, only a small fraction of the water was measured to be in the air.

Two different mechanisms of blast suppression are proposed by Schwer et al. [24] and Ananth et al. [22], however they both suggest suppression is achievable with mist and that greater suppression is achieved with higher mist concentrations. Detonation experiments in Figures 13 and 14 along with the overpressure results in Table 7 once again emphasize that the mist conditions that produced the highest measured concentration of water in the chamber had the greatest effect on suppressing the overpressures produced by the detonation of TNT and PBXN-109. The impulse, initial blast wave, and quasi-static peak pressures for TNT and PBXN-109 were suppressed by (40%, 36%, 35%) and (49%, 39%, 41%) compared to (26%, 16%, 28%) and (9%, 16%, 20%) suppression using less water (Table 7).
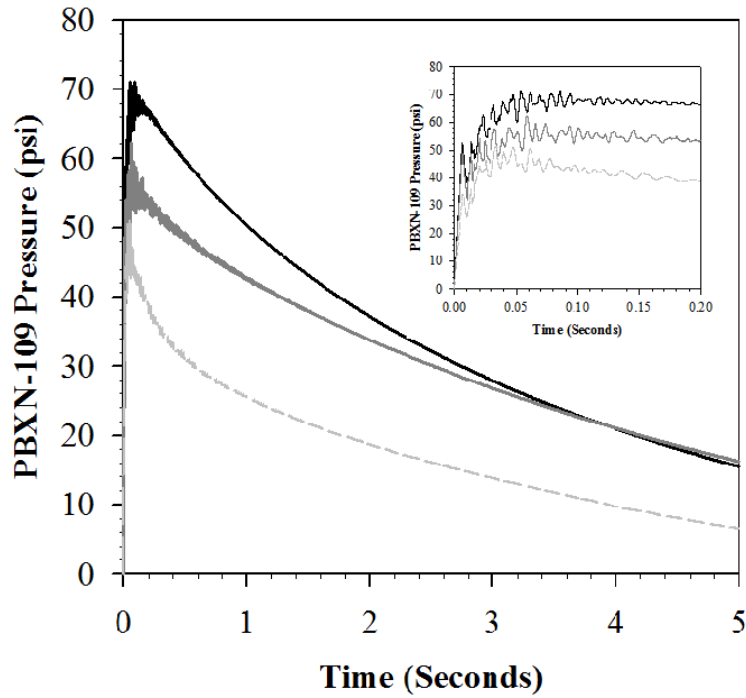
Figure 13. 50 lbs equivalent PBXN-109 Smoothed Pressure Trace with and without water mist: Black (baseline), Light Grey (--- Nozzle set 1 (100 bar)), Dark Grey (─ Nozzle set 3 (100 bar)).
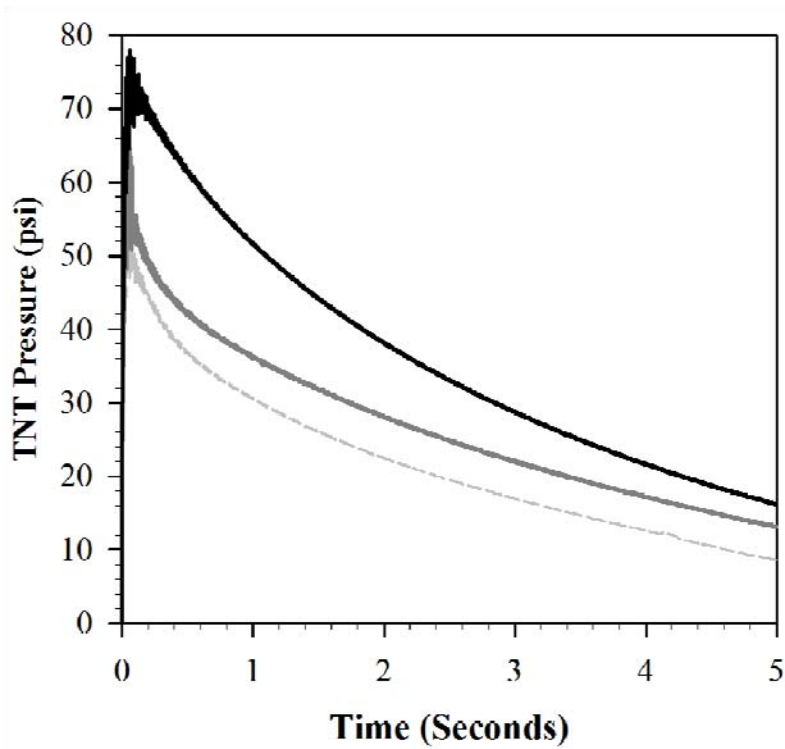

Figure 14. 50 lbs TNT Smoothed Pressure Trace with and without water mist: Black (baseline), Light Grey (--- Nozzle set 1 (100 bar)), Dark Grey (─ Nozzle set 1 (35 bar)).

9.0   CONCLUSIONS

Blast mitigation experiments were conducted in a vented chamber using three different HE explosives, TNT, Destex, and PBXN-109. The mist produced by 3 separate nozzle sets operating under different conditions was characterized prior to the detonation experiments. The impulse, initial blast wave, and quasi-static overpressure generated by the detonations were reduced by as much as (40%, 36%, 35%) for 50 lbs TNT, (43%, 25%, 33%) for 50 lbs TNT equivalent Destex, and (49%, 39%, 41%) for 50 lbs equivalent PBXN-109 using water mist at concentrations and drop sizes of 70 g/m^3 and 54 μm SMD. These suppression results are similar to those achieved for the low charge density (2 lbs, 5 lbs, and 7 lbs TNT) explosion experiments conducted in 2005 at NSWC Indian Head, Maryland. This suggests suppression is scalable to larger charges. In addition the mist characterization studies indicate the mist conditions reach steady state output within seconds of initiating the mist into the chamber. Therefore the preemptive application of water mist at concentrations and droplet sizes typically employed for fires suppression could lead to significant suppression against HE explosives used in military application and terrorist attacks.

The suppression results obtained for the aluminized explosives, Destex and PBXN-109 were comparable to the amount of suppression of the impulse, initial blast wave, and quasi-static peak pressure measured for TNT using the highest mist density (70 g/m^3) conditions. These results substantiated thermodynamic calculation that predicted a reduction in overpressures with the application of water mist [22].

The measured mist droplet concentrations used in this test series (70 g/m^3, 57 g/m^3, 29 g/m^3) and the previous test series (87 g/m^3) along with the suppression results appear to support Navier-Stokes simulations performed by Ananth et al [22] and the experimental results found by Thomas et al. [25] that suggest latent heat absorption by evaporation is the primary mechanism behind explosion suppression in a confined space.

Finally the results of the detonation experiments with TNT and PBXN-109 showed that the highest mist density conditions (70 g/m^3) outperformed lower mist concentrations produced in the chamber (57 g/m^3, 29 g/m^3). This difference in the suppression of the impulse, initial blast wave, and quasi-static peak pressure using different mist densities in the detonation experiments corroborate simulations by Schwer et al and Ananth et al that suggest greater suppression is achieved with higher mist concentrations in a confined space.

10.0   ACKNOWLEDGMENTS

11.0   REFERENCES

1. G. G. Back, P. J. DiNenno, J. T. Leonard, R. L. Darwin, "Full Scale Tests of Water Mist Fire Suppression Systems for Navy Shipboard Machinery Spaces: Phase I – Unobstructed Spaces," NRL Memorandum Report 6180-96-7830, 8 March 1996.

2. G. G. Back, P. J. DiNenno, J. T. Leonard, R. L. Darwin, "Full Scale Tests of Water Mist Fire Suppression Systems for Navy Shipboard Machinery Spaces: Phase II – Obstructed Spaces," NRL Memorandum Report 6180-96-7831, 8 March 1996.

3. F. W. Williams, G. G. III Back, P. J. DiNeeno, R. L. Darwin, S. A. Hill, B. J. Havlovick, T. A. Toomey, J. P. Farley, J. M. Hill, "Full-Scale Machinery Space Water Mist Test: Final Design Validation," NRL Memorandum Report 6180-99-8380, 12 June 1999.

4. K. Kailasanath, P. A. Tatem, F. W. Williams, J. Mawhinney, "Blast Mitigation Using Water-A Status Report," NRL Memorandum Report 6410-02-8606, 15 March 2002.

5. D. Schwer, K. Kailasanath, "Blast Mitigation by Water Mist (1) Simulation of Confined Blast Waves," NRL Memorandum Report 6410-02-8636, 16 August 2002.

6. D. Schwer, K. Kailasanath, "Blast Mitigation by Water Mist (2) Shock Wave Mitigation Using Glass Particles and Water Droplets in Shock Tubes," NRL Memorandum Report 6410-02-8658, 21 January 2003.

7. G. O. Thomas. "On the Conditions Required for Explosion Mitigation by Water Sprays," *Trans IChemE Part B*, **2000**, 78, 339-354.

8. K. van Wingerden, "Mitigation of Gas Explosions Using Water Deluge," *Process Safety Progress*, **2000**, 19, 173-178.

9. C. Catlin, "Passive explosion suppression by blast-induced atomization from water containers," J. Hazardous Materials, **2002**, A94, 103-132.

10. W. A. Keenan, P. C. Wager, "Mitigation of Confined Explosion Effects by Placing Water in Proximity of Explosives," 25th DOD Explosives Safety Seminar, Anaheim, CA, August 18-20, 1992.

11. M. H. Keshavarz, "New Method for Predicting Detonation Velocities of Aluminized Explosives," *Combust. Flame*, **2005**, 142, 303-307.

12. OPNAV P-86-4-99, "U.S. Navy Survivability Design Handbook for Surface Ships", September 2000. CNO-N86DC

13. J. L. Bailey, M. S. Lindsay, D. A. Schwer, J. P. Farley, and F. W. Williams, "Blast Mitigation Using Water Mist," NRL Memorandum Report 6180-06-8933, 18 January 2006.

14. H. D. Willauer, J. L. Bailey, F. W. Williams, "Water Mist Suppression System Analysis," NRL Letter Report 6180/0030, 7 February 2006.

15. A. H. Lefebvre "Atomization and Sprays," Hemisphere Publishing Corporation: Philadelphia, 1988.

16. H. D. Willauer, R. Ananth, J. P. Farley, F. W. Williams, G. G. Back, M. C. Kennedy, V. M. Gameiro "Revised Test Plan: Blast Mitigation Using Water Mist" NRL Letter Report 6180/0194, 23 May 2007.

17. globalsecurity.org/military/systems/munitions/explosives.htm (accessed September 2008).

18. P. W. Cooper, "Explosives Engineering," Wiley-VCH publisher, 1996.

19. J. W. Kury, R. D. Breithaupt, and C. M. Tarver, "Detonation Waves in Trinitrotoluene," *Shock Waves*, **1999**, 9, 227-237.

20. S. D. Gilev and V. F. Anisichkin, "Interaction of Aluminum with Detonation Products," *Combust., Exp., and Shock Waves*, **2006**, 42, 107-115.

21. K. C. Adiga, H. D. Willauer, R. Ananth, F. W. Williams, "Droplet Breakup Energies and Formation of Ultra-Fine Mist, "NRL Memorandum Report 6180-06-8985, 13 September 2006.

22. R. Ananth, H. D. Ladouceur, H. D. Willauer, J. P. Farley, F. W. Williams "Effect of Water Mist on a Confined Blast" Presented before the Suppression and Detection Research and Applications- A Technical Working Conference (SUPDET 2008) (March 11-13, 2008) Orlando, Florida.

23. D. Tassia, K. Rye, "Internal Blast Testing of Explosives for Use in Large Diameter Bombs and Missiles," OJTR 2038, NSWC Indian Head, 26 February 1998.

24. D. Schwer, K. Kailasanath, "Blast Mitigation by Water Mist (3) Mitigation of Confined and Unconfined Blasts," NRL Memorandum Report 6410-06-8976, 14 July 2006.

25. G. O. Thomas, A. Jones, M. J. Edwards, Influence of Water Sprays on Explosion Development in Fuel-Air Mixtures, *Combust. Sci. and Tech.*, **1991**, 80, 47-61.

APPENDIX A.

Table A-1. Nozzle Properties

Nozzle	Number	Location	Conditions	Con (g/m³)	Dv(10) (μm)	Dv(50) (μm)	Dv(90) (μm)	SMD (μm)
4S 1MC 8MB	A4	Center 91	100 bar	67.1	57.2	165.2	327.0	48.1
	A5	Center 91	100 bar	70.5	52.4	165.1	332.1	54.1
	A1	Center 25	100 bar	52.3	75.1	229.5	387.0	46.4
	A2	Center 25	100 bar	71.5	57.6	215.9	384.9	54.9
	A7	Back R 91	100 bar	54.4	38.4	159.5	330.2	40.9
	A3	Front R 25	100 bar	62	99.1	237.2	386.0	119.2
	A20	Center 91	35bar	61.7	71.4	182.4	334.8	108.0
	A21	Center 91	35bar	52.3	70.4	186.1	334.7	102.7
4S 1MC 8MB (Hybrid)	A19	Center 91	100 bar (hybrid)	33.8	12.8	73.6	193.4	24.9
	A22	Center 91	100 bar (hybrid)	37.3	12.8	87.4	253.7	28.4
3N 1MA 4MA	A10	Center 91	100 bar	27.5	63.5	176.4	337.2	80.7
	A23	Center 91	100 bar	30.2	65.8	173.7	328.5	86.5
	A8	Center 25	100 bar	37.8	102.3	22.2	346.9	151.2
	A12	Back R 91	100 bar	26.6	70.9	190.4	352.2	88.1
	A9	Front R 25	100 bar	18.5	98.8	244.4	389.4	97.9
4S 1MB 6MB	A15	Center 91	100 bar	58.5	6.4	147.4	336.7	30.1
	A17	Center 91	35 bar	46.9	67.9	205.4	362.8	115.8
	A13	Center 25	100 bar	54.5	91.4	213.0	367.1	125.7
	A14	Front R 25	100 bar	47.5	92.1	217.5	370.2	123.3